EARTHQUAKE ENGINEERING AND STRUCTURAL DYNAMICS
Earthquake Engng Struct. Dyn. 2000; **29**:1131–1152

Bayesian probabilistic damage detection of a reinforced-concrete bridge column

Hoon Sohn[1,*,†] and Kincho H. Law[2]

[1] *Engineering Sciences and Applications Division, Engineering Analysis Group, Los Alamos National Laboratory, NM 87545, U.S.A.*
[2] *Department of Civil and Environmental Engineering, Stanford University, Stanford, CA 94305, U.S.A.*

SUMMARY

A Bayesian probabilistic approach for damage detection has been proposed for the continuous monitoring of civil structures (Sohn H, Law KH. Bayesian probabilistic approach for structure damage detection. *Earthquake Engineering and Structural Dynamics* 1997; **26**: 1259–1281). This paper describes the application of the Bayesian approach to predict the location of plastic hinge deformation using the experimental data obtained from the vibration tests of a reinforced-concrete bridge column. The column was statically pushed incrementally with lateral displacements until a plastic hinge is fully formed at the bottom portion of the column. Vibration tests were performed at different damage stages. The proposed damage detection method was able to locate the damaged region using a simplified analytical model and the modal parameters estimated from the vibration tests, although (1) only the first bending and first torsional modes were estimated from the experimental test data, (2) the locations where the accelerations were measured did not coincide with the degrees of freedom of the analytical model, and (3) there existed discrepancies between the undamaged test structure and the analytical model. The Bayesian framework was able to systematically update the damage probabilities when new test data became available. Better diagnosis was obtained by employing multiple data sets than just by using each test data set separately. Copyright © 2000 John Wiley & Sons, Ltd.

KEY WORDS: damage detection; Bayesian probabilistic approach; continuous monitoring; vibration test; bridge column structure

1. INTRODUCTION

The monitoring of civil structures has received increasing interest in the research community. There have been increased economic and societal demands to periodically monitor the safety of

* Correspondence to: Hoon Sohn, Engineering Sciences and Applications Division, Engineering Analysis Group, ESA-EA MS-C926, Los Alamos National Laboratory, Los Alamos, NM 87545, U.S.A.
† E-mail: sohn@lanl.gov.

Received 29 June 1998
Revised 27 January 2000
Accepted 15 February 2000

structures against long-term deterioration, and to immediately assess the condition after extreme events such as earthquakes. The condition assessment of civil structures after extreme events is of great importance for emergency management officials to properly allocate resources for prompt emergency response. An equally important task is the continuous/periodic monitoring of civil structures to ensure their safety and adequate performance during the life span of the structures.

Many of the existing damage detection and monitoring algorithms [1–3] have originally been developed in the field of aerospace industry for the monitoring of space-station-like structures such as truss structures. These algorithms do not fully address the issues that arise in the monitoring of civil structures. The main challenges for the development of a robust damage detection and monitoring system for civil structures are as follows:

1. Civil structures involve a significant amount of uncertainties caused by environmental effects such as temperature, loading, humidity, and so on. For example, an experimental study shows that several concrete bridges in the United Kingdom absorbed considerable amount of moisture during damp weather, and consequently increased the mass of the bridge [4]. Also, experimental modal analysis conducted on the Alamosa Canyon Bridge reveals that the ambient temperature could cause more than 5 per cent variation in the estimated fundamental frequency within a 24 hour period [5, 6]. These changes are shown possibly to be several times the modal property changes expected from structural damage. In addition, the uncertainty to estimate the strength and stiffness of structural components is significantly higher than that of truss members commonly used for space structures.
2. Civil structures typically display more complicated geometry; consist of many different materials such as steel, concrete, cable and asphalt; and involve more redundancy in the design than space structures. These issues make the accurate modeling of civil structures very difficult. Model updating and refinement techniques [7–10] can be employed prior to damage detection. However, the practical applications of these techniques primarily are to research activities. Model updating and refinement techniques assume that the degrees of freedom (DOFs) of the measured modal vectors match identically to the DOFs of the analytical model. This assumption can be met when measurements are conducted at all DOFs of the analytical model, or when mode shape expansion or model reduction techniques are employed. However, the mode shape expansion and model reduction techniques introduce significant errors into the model refinement procedure if the measurements are limited to small number of locations. Furthermore, many model updating techniques utilize the connectivity information of the structural members to obtain a better baseline model. On the other hand, the connectivity information is lost when model reduction is applied. Last but not least, it is known that model updating could produce multiple, nonunique models [11, 12].
3. The size of civil structures does not permit the instrumentation of a large number of sensors and actuators, and the excitation of higher modes. Furthermore, the application of forced vibration tests, which are commonly used for system identification, is difficult for civil structures in service because of the economic and social ramification caused by service interruption due to road closure and evacuation of buildings. Ambient vibration tests are more suitable for civil structures since the test can be conducted under normal operation of structures and can be easily repeated to collect additional modal data sets. One difficulty

with ambient tests is the difficulty of exciting higher modes. Therefore, most damage detection for civil structures would suffer from lack of data: only a small number of measurement points and a few fundamental modes would be available.

To overcome the aforementioned problems, the authors proposed a damage detection method particularly aimed at the continuous monitoring of civil structures [13, 14]. The proposed method is a probability-based approach, that is more attractive to civil structures than the existing deterministic approaches, and is a model-based approach that does not necessarily require an accurate analytical model. The proposed Bayesian probabilistic approach offers the following potential advantages: (1) it takes into account the uncertainties in the measurement noise and the analytical modelling, (2) it is able to perform damage detection when only a small number of degrees of freedom are measured and a few modes are estimated, and (3) it systematically extracts information from the continuously obtained test data. An experimental investigation for the proposed Bayesian approach is conducted in this paper. The proposed Bayesian approach is applied to locate the plastic hinge of a concrete bridge column based on the data obtained from the vibration tests conducted at the University of California, Irvine (UCI).

This paper is organized as follows. Section 2 briefly reviews the Bayesian-based damage detection approach. Section 3 describes the experimental setup of the column test at UCI. Section 4 presents the analytical modeling of the column structure and compares the measured and analytical modal parameters. Section 5 applies the proposed Bayesian approach to the detection of the plastic hinge location. Section 6 summarizes this paper and discusses further work.

2. THEORETICAL FORMULATION

This section briefly reviews the Bayesian framework for damage detection described in Reference [13]. The idea is to search for the most probable damage event by comparing the relative probabilities for different damage scenarios, where the relative probability of a damage event is expressed in terms of the posterior probability of the damage event, given the estimated modal data sets from a structure. The formulation of the relative posterior probability is based on an output error, which is defined as the difference between the estimated modal parameters and the theoretical modal parameters from the analytical model.

For an analytical model of a structure, we represent the system stiffness matrix $\mathbf{K}$ as an assembly of substructure stiffness matrices. For a model with N_{sub} substructures, the overall stiffness matrix can be expressed as

$$\mathbf{K}(\Theta) = \sum_{i=1}^{N_{\text{sub}}} \theta_i \mathbf{K}_{si} \tag{1}$$

where $\mathbf{K}_{si}$ is the stiffness matrix of the ith substructure and θ_i $(0 \leqslant \theta_i \leqslant 1)$ is a non-dimensional parameter that represents the contribution of the ith substructure stiffness to the system stiffness matrix. The non-dimensional parameter θ_i is introduced to allow the modelling of damage in the ith substructure. A substructure is defined as *damaged* when the θ value is less than a specified threshold. As damage locations and amount are determined according to the θ values, the system stiffness matrix in Equation (1) is expressed as a function of $\Theta = \{\theta_i;\ i, \ldots, N_{\text{sub}}\}$.

Test data sets are assumed to be collected from repeated vibration tests. When vibration tests are repeated N_s times, the total collection of N_s data sets is denoted

$$\hat{\Psi}_{N_s} = \{\hat{\psi}(n): n = 1, \ldots, N_s\} \tag{2}$$

A modal data set $\hat{\psi}(n)$ in Equation (2) consists of both the frequencies and the modal vectors estimated from the nth vibration test, i.e.

$$\hat{\psi}(n) = [\hat{\omega}_1^n, \ldots, \hat{\omega}_{N_m}^n, \hat{\mathbf{v}}_1^{n\mathrm{T}}, \ldots, \hat{\mathbf{v}}_{N_m}^{n\mathrm{T}}]^{\mathrm{T}} \in \mathbf{R}^{N_t} \tag{3}$$

where $\hat{\omega}_i^n$ and $\hat{\mathbf{v}}_i^n$ denote, respectively, the ith estimated frequency and modal vector in the nth data set. The modal vector $\hat{\mathbf{v}}_i^n$ ($\in \mathbf{R}^{N_d}$) has components corresponding to the instrumented DOFs. The variables N_t, N_d, and N_m represent the total number of components in a data set $\hat{\psi}(n)$, the number of the measured DOFs, and the number of the estimated modes, respectively.

Let H_j denote a hypothesis for a damage even that can contain any number of substructures as damaged, and the initial degree of belief about the hypothesis H_j is represented with a prior probability $P(\mathrm{H}_j)$. Using Bayes' theorem, the posterior probability $P(\mathrm{H}_j | \hat{\Psi}_{N_s})$, after observing the estimated data sets $\hat{\Psi}_{N_s}$, is given by

$$P(\mathrm{H}_j | \hat{\Psi}_{N_s}) = \frac{P(\hat{\Psi}_{N_s} | \mathrm{H}_j)}{P(\hat{\Psi}_{N_s})} P(\mathrm{H}_j) \tag{4}$$

The most likely damaged substructures are the ones included in the hypothesis $\mathrm{H}_{\max}$ which has the largest posterior probability, i.e.

$$P(\mathrm{H}_{\max} | \hat{\Psi}_{N_s}) = \max_{\forall \mathrm{H}_j} P(\mathrm{H}_j | \hat{\Psi}_{N_s}) \tag{5}$$

Since the objective is to determine the most probable damage hypothesis (event), only the relative posterior probabilities of alternative hypotheses are of interest. We attempt to avoid the explicit expression of a posterior probability $P(\mathrm{H}_j | \hat{\Psi}_{N_s})$ since the precise calculation of $P(\hat{\Psi}_{N_s} | \mathrm{H}_j)$ is a difficult task. To overcome these difficulties, we focus on the relative comparisons of posterior probabilities.

After some mathematical simplifications, one can show that the most probable hypothesis $\mathrm{H}_{\max}$ in Equation (5) satisfies [13]:

$$J(\hat{\Psi}_{N_s}, \Theta_{\mathrm{H}_{\max}}^{\max}) - \ln P(\mathrm{H}_{\max}) = \min_{\forall \mathrm{H}_j} [J(\hat{\Psi}_{N_s}, \Theta_{H_j}^{\max}) - \ln P(\mathrm{H}_j)] \tag{6}$$

where ln denotes a natural logarithm and an analytical modal data set $\psi(\Theta_{\mathrm{H}_j})$ for a given Θ_{H_j} is defined similar to Equation (3):

$$\psi(\Theta_{H_j}) = [\omega_1(\Theta_{\mathrm{H}_j}), \ldots, \omega_{N_m}(\Theta_{\mathrm{H}_j}), \mathbf{v}_1^{\mathrm{T}}(\Theta_{\mathrm{H}_j}), \ldots, \mathbf{v}_{N_m}^{\mathrm{T}}(\Theta_{\mathrm{H}_j})]^{\mathrm{T}} \in \mathbf{R}^{N_t} \tag{7}$$

Furthermore, the error function $J(\hat{\Psi}_{N_s}, \Theta_{\mathrm{H}_j})$ is given by

$$J(\hat{\Psi}_{N_s}, \Theta_{\mathrm{H}_j}^{\max}) = \frac{1}{2} \sum_{n=1}^{N_s} [\hat{\psi}(n) - \psi(\Theta_{\mathrm{H}_j}^{\max})]^{\mathrm{T}} \mathbf{C}_{\Psi}^{-1} [\hat{\psi}(n) - \psi(\Theta_{\mathrm{H}_j}^{\max})] \tag{8}$$

where the most probable parameter values $\Theta_{\mathrm{H}_j}^{\max}$ maximize the conditional probability density function $f(\Theta_{\mathrm{H}_j} | \hat{\Psi}_{N_s})$ for a given hypothesis H_j, and $\| \mathrm{C}_{\Psi} \| = \det | \mathrm{diag}[\sigma_1^2, \ldots, \sigma_{N_t}^2] | = \prod_{i=1}^{N_t} \sigma_i^2$.

When a large number of experimental data sets are available, the variance σ_i^2 can be easily estimated from the data set. Recently, a technique has been proposed to estimate the uncertainties in the modal parameters even when available modal data sets are small [15]. Such technique can potentially be incorporated in the Bayesian framework described. However, in this study, a uniform coefficient of variation (COV) is simply assigned to all modal parameters. Now, the comparison of posterior probabilities can be conducted by examining only the error function $J(\hat{\Psi}_{N_s}, \Theta_{\mathbf{H}_j}^{\max})$ and the prior probability $P(\mathrm{H}_j)$. In Reference [13], additional modelling error term is included in Equation (8), and the modelling error is quantified using multiple sets of modal parameters from the undamaged structure. However, since only a single set of modal parameters are available from the undamaged structure in this study, the modelling error is minimized by adjusting the initial analytical model, and left out from the formulation of the error function in Equation (8). Finally, a branch-and-bound search scheme is proposed to expedite the search for the most likely damaged substructure without exhaustively examining all the possible damage cases [13].

3. DESCRIPTION OF EXPERIMENTAL SET-UP

This damage detection study is based on the experimental tests of bridge columns conducted at the University of California, Irvine. The test structure consisted of two concrete bridge columns, the diameter of which was retrofitted from 24 in (61.0 cm) to 36 in (91.4 cm). The first column was retrofitted by placing forms around the existing column and placing additional concrete within the form. The diameter of second column was extended by spraying concrete in a process referred to as shotcreting. The shotcreted column was then polished with a trowel to obtain a circular cross-section. Incremental cyclic load tests were performed on the bridge columns with and without the retrofit procedures. Static lateral loads were incrementally applied to the top of a column until the ultimate load capacity of the column was reached. The column was cycled three times after each load increment and modal analysis was conducted after each cyclic load testing. The experimental modal analysis of the columns was performed by the Engineering Analysis Group of the Los Alamos National Laboratory (LANL).[‡] The vibration test data obtained from the first column were employed for modal analysis and damage detection in this study.

Figure 1 shows the configuration of the test column. The column employed in this study was cast on top of a 56 in^2 (361.3 cm^2) concrete foundation with a height of 25 in (63.5 cm). A 25 in^2 (161.3 cm) concrete block was cast on the top of the column, and a hydraulic actuator for the static cyclic testing and an electro-magnetic shaker for the modal analysis were attached to this block. As is typical of actual retorfit in the field, a 1.5 in (3.8 cm) gap was left between the top of the foundation and the bottom of the increased column part. Therefore, the vertical reinforcement in the retrofitted portion of the column did not extend into the foundation. Since the concrete foundation was bolted to the laboratory floor, the bottom of the foundation was not moved once testing started. An inner circle of 10 #6 vertical rebars with a yield strength of 74.9 ksi (516.4 MPa) were embedded within the initial 24 in (61.0 cm) column. These rebars were enclosed

[‡] A detailed description of the columns and the data obtained from the tests are provided on the web site 'http://esaea-www.esa.lanl.gov/damage_id'.

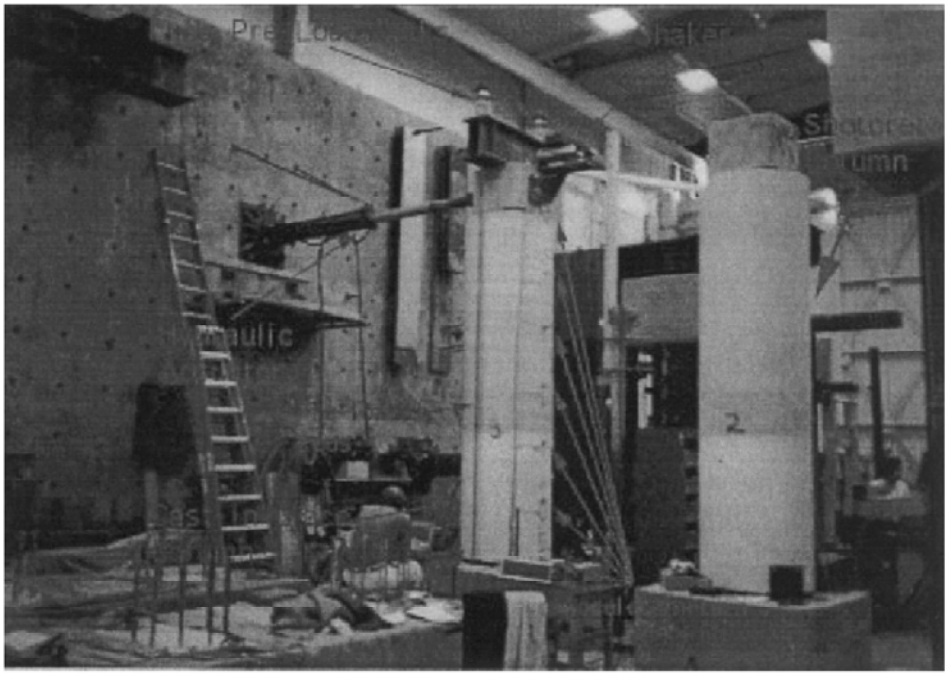

Figure 1. UC Irvine test configuration (Courtesy of the Los Alamos National Laboratory).

by a spiral cage of #2 rebars with a yield strength 30 ksi (206.9 MPa) and spaced at 7 in (17.8 cm) pitch. The retrofit jacket had 16 #8 vertical rebars with a yield strength of 60 ksi (414.0 MPa). These rebars were enclosed by a spiral cage of #6 rebars spaced at 6 in (15.2 cm) pitch.

Cyclic lateral loads were applied to the top of the column using an hydraulic actuator. The loads were first applied in a force-controlled manner to produce lateral deformations at the top of the column, corresponding to $0.25\Delta y_T$, $0.5\Delta y_T$, $0.75\Delta y_T$, and Δy_T, respectively. Here Δy_T is the lateral deformation corresponding to the theoretical first yield of the longitudinal reinforcement. The structure was cycled three times at each load level. Based on the observation of these responses under force-controlled loadings, a lateral deformation corresponding to the actual first yield, Δy, was calculated.[§] Next, the loading was increased in a displacement-controlled manner corresponding to Δy, $1.5\Delta y$, $2.5\Delta y$, $4.0\Delta y$ and $7.0\Delta y$, respectively. The incremental loadings caused continuous deterioration of the column stiffness. The formation of a plastic hinge was observed between the top of the foundation and the bottom of the retrofit jacket.

For the modal analysis, the column was excited by an APS electro-magnetic shaker mounted at the top of the column, and the shaker was mounted off the axis to excite torsional modes. The shaker rested on a steep plate attached to the concrete top. Note that the actuator was operated in an open-loop mode and there was a significant feedback to the actuator through the steel plate.

[§] A detailed summary of the calculation of the actual first yielding deformation can be found in 'http://www.ics.uci.edu/ ~ athomas/caltrans'.

This feedback resulted in a poor band-limited white noise excitation to the column and rendered the identification of modal parameters difficult.

The exciting force was measured with an accelerometer mounted to the sliding mass of the shaker 0.18 lb s^2/in (31.5 kg). The same magnitude of excitation was used in all tests. Figure 2 shows the locations of the forty accelerometers mounted. Locations 2, 39, and 40 had PCB 302A

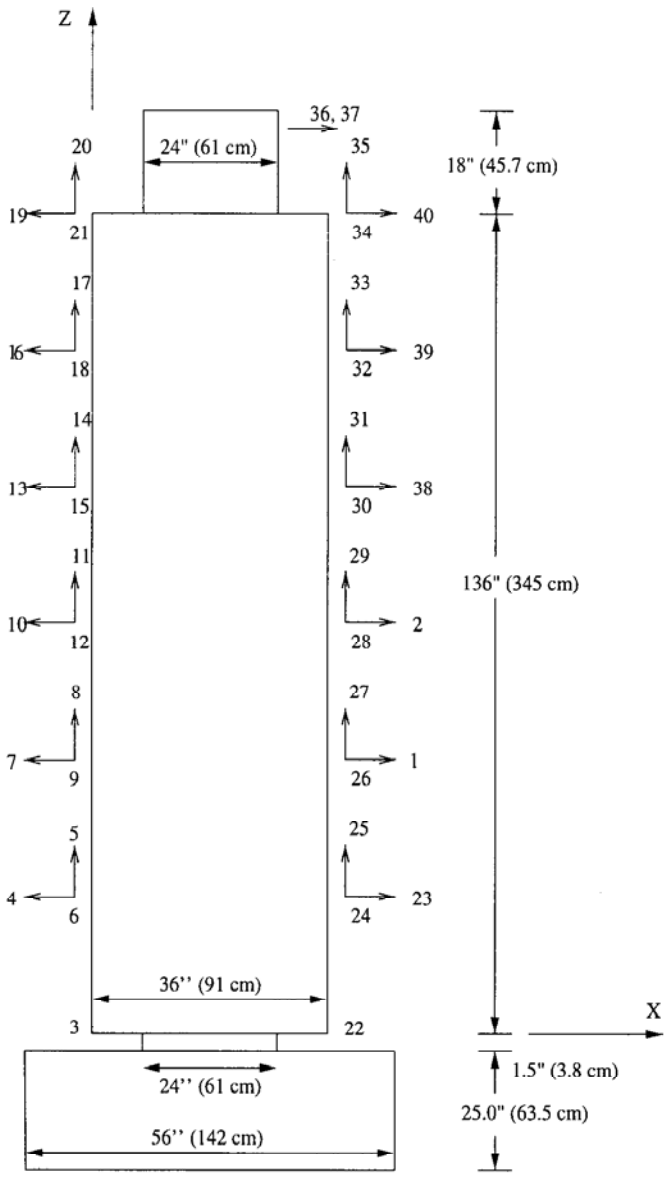

Figure 2. Dimensions and accelerometer locations of UC Irvine column test.

accelerometers with a nominal sensitivity 10 mV/g. Since these accelerometers were found not to be sensitive enough to measure the desired vibration quantities, the acceleration data from these sensors were excluded for modal analysis. Wilcoxon 736t accelerometers with a nominal sensitivity of 100 mV/g were placed in locations 33, 34, 35, 36 and 37. All other locations had PCB 336C accelerometers with a nominal sensitivity of 1 V/g. Accelerometers 36 and 37 were located 8 in (20.3 cm) off the axis in the y direction.

Data were sampled and processed with an HP 3566A dynamic data acquisition system. Frequency response functions (FRFs), auto and cross power spectra, and coherence functions were measured in the range of 0–400 Hz. Each spectrum was calculated from 30 averages of 2 s duration time histories with 2048 sampling points. This sampling rate produced a frequency resolution of 0.5 Hz. Time history measurements and FRF analysis were conducted after each cyclic load test was done at the deformation levels, Δy, $1.5\Delta y$, $2.5\Delta y$, $4.0\Delta y$, and $7.0\Delta y$, respectively. For simplicity, the tests corresponding to the deformation level, Λy, $1.5\Lambda y$, $2.5\Lambda y$, $4.0\Lambda y$, and $7.0\Delta y$, are labelled hereafter as Test 1, Test 2, Test 3, Test 4, and Test 5, respectively. Furthermore, the vibration test prior to any cyclic loading is referred to as Test 0.

4. ANALYTICAL MODELING

Two analytical models are constructed for damage detection. The first model (Model 1) consists of 9 beam elements and the second model (Model 2) had 27 beam elements (see Figures 3 and 4). Each node of a beam element contains three translational DOFs and three rotational DOFs. Therefore, Models 1 and 2 have a total of 54 and 162 DOFs, respectively. An elastic modulus of 3.6×10^6 psi (2.48×10^4 MPa), a mass density of 2.17×10^{-4} lb s^2/in^4 (2.32×10^{-3} kg/cm^3), and a Poission's ratio of 0.2 are specified in the models. The DOFs at the base of the foundation were constrained for translation and rotation.

To construct the system mass matrix, the lumped mass m and the mass moments of inertia I^M are computed as: $m = \gamma \times \pi r^2 \times h$, I_x^M, $I_y^M = \frac{1}{12} m(3r^2 + h^2)$ and $I_Z^M = \frac{1}{2} mr^2$. Here, γ is a mass density of 2.17×10^{-4} lb s^2/in^4 (2.32×10^{-3} kg/cm^3), r is the radius of the column, and h is the height of the tributary area. Furthermore, the masses of the actuator and the steel plate are added to the top node of the column (Node 10 in Figure 3 and Node 28 in Figure 4, respectively). Next, the analytical models are refined based on engineering judgment to match the measured model parameters rather than employing model updating techniques. Model updating techniques are not employed because of the following reasons:

1. The model updating techniques are primarily used to update the design parameters such as elastic moduli, cross-sectional area and so on. However, They are unable to update boundary conditions nor the configuration of a structure.
2. When the measurement points do not coincide with the DOFs of the analytical modal (which is the case in this experimental study), the model updating techniques are difficult to apply.
3. Many updating techniques focus on the stiffness updating. However, in this experimental study, good estimates of the mass and the mass moment of inertia are essential.

Refinements made to the analytical models are mainly focused on the consideration of the reinforcement steel, the estimation of the mass moments of inertia of the steel plate and the

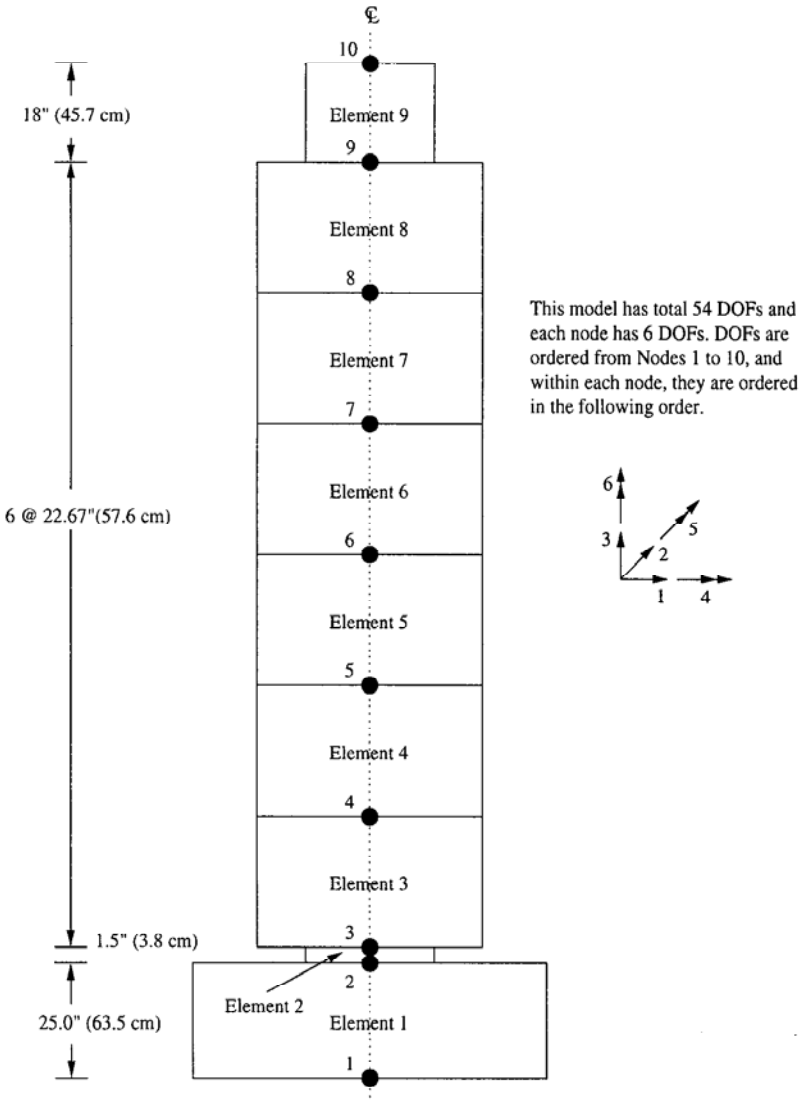

Figure 3. Analytical Model 1 of UC Irvine column test.

actuator, and the connection modelling between the foundation and the column. It should be noted that there may exist multiple updated models. The non-uniqueness issue in model updating is addressed in References [11, 12] and the corresponding Bayesian approach is formulated in References [16, 17]. Because the computational effort involved with multiple models could become prohibitive, a single updated model is employed in this study to illustrate the applicability of the proposed approach.

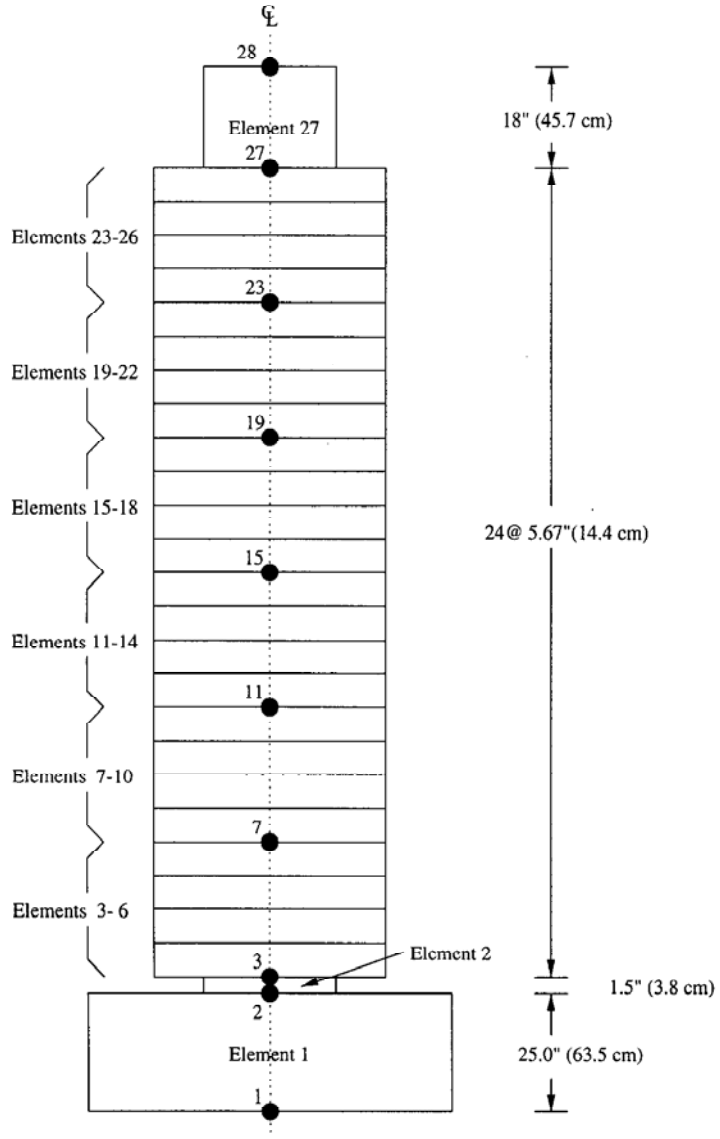

Figure 4. Analytical Model 2 of UC Irvine column test.

The natural frequencies from the test data and two analytical models are summarized in Table I. Table I shows the first three bending modes in the X direction, the first two torsional modes, and first axial mode. The second column of Table I shows the estimated natural frequencies from the experimental modal analysis of the undamaged column (Test 0). The experimental modal analysis fails to identify the first axial mode. The natural frequencies

Table I. Natural frequency (Hz) from the analytical models.

	Test 0	Model 1*	Model 2*	Model 3†	Model 4†
1st bending	27.82	26.55	25.38	19.10	25.60
1st torsion	110.42	115.87	116.04	114.00	131.00
2nd bending	147.51	150.62	146.37	124.00	136.00
1st axial	—	206.36	201.35	181.00	204.00
2nd torsion	272.83	276.04	276.63	351.00	389.00
3rd bending	340.71	374.03	362.36	306.00	319.00

* Models 1 and 2 are shown in Figures 3 and 4, respectively.
† Models 3 and 4 are constructed at the Los Alamos National Laboratory.

obtained from Models 1 and 2 are also tabulated. In addition, the natural frequencies of two additional models (Models 3 and 4) are constructed at the LANL using a finite element analysis software, ABAQUS. Model 3 is constructed using 8-node continuum elements and has 20 979 DOFs. Model 4 is constructed using three-node beam elements and has 114 DOFs. Reinforcement is not incorporated in the LANL models. Because of the symmetry of the column, identical bending modes occur in both X and Y directions at the same natural frequencies. Only the bending modes in the X direction are presented here.

Note that the order of the second torsion and third bending modes in Models 1 and 2 is switched for Models 3 and 4. It appears that the differences between the models in this study (Models 1 and 2) and the LANL models (Models 3 and 4) arise mainly from the differences in the consideration of reinforcement, the addition of actuator and steel plate masses, and the computation of the mass moment of inertia. We can observe that since the reinforcement is included in Models 1 and 2, the bending mode frequencies of these models are higher than those of the LANL models. In contrast, the torsional mode frequencies in the LANL models are higher than those of Models 1 and 2. The inclusion of the actuator and steel plate masses, and the mass moment of inertia computed for Models 1 and 2 seem to have lowered the frequencies of corresponding torsional modes. In the next section, only Models 1 and 2 are employed for damaged detection.

Since the measurement points on the test column do not coincide with the DOFs of the analytical models, the displacement at the measurement points are reconstructed at the DOFs of the analytical model. Figure 5 shows the displacement transformation matrix that relates the acceleration measurement points (X_l, Y_l, Z_l, X_r, Y_r and Z_r) to the DOFs of the analytical model (X_c, Y_c, Z_c, R_x, R_y and R_z). All measured modal vectors are reconstructed at the analytical DOFs after the displacement transformation. However, it should be noted that there are not sufficient accelerometers placed to reconstruct the estimated modal vectors at all the DOFs in the analytical model. That is, the components of the estimated modal vectors corresponding to nodes 2, 3 and 10 in the analytical model of Figure 3 could not be obtained from the measurement points. For a graphical display of the measured modal vectors, the uninstrumented DOFs corresponding to the nodes 2, 3 and 10 in Figure 3 are simply assumed to be identical to adjacent nodes. For example, the displacements at nodes 2, 3 and 10 are set identical to the displacements at nodes 1, 4 and 9, respectively. Figures 6–9 show the analytical and measured modal vectors corresponding to the first bending and the first torsional modes in Table I. The analytical modal vectors in Figures 6 and 8 are computed from Model 1 in Figure 3. The measured modal vectors in Figures 7 and 9 are computed from Test 0.

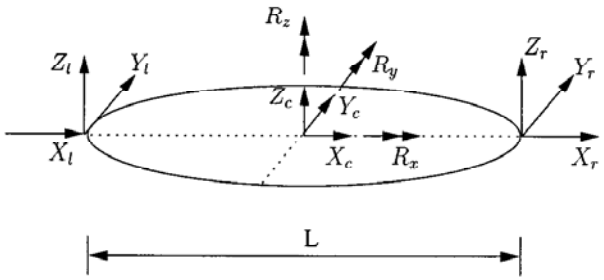

(a) The acceleration measurement points and the DOFs of the analytical model

$$\begin{Bmatrix} X_c \\ Y_c \\ Z_c \\ R_x \\ R_y \\ R_z \end{Bmatrix} = \begin{bmatrix} 1/2 & & & 1/2 & & \\ & 1/2 & & & 1/2 & \\ & & 1/2 & & & 1/2 \\ 1/L & & & -1/L & & \\ & & 1/L & & & -1/L \\ & -1/L & & & 1/L & \end{bmatrix} \begin{Bmatrix} X_l \\ Y_l \\ Z_l \\ X_r \\ Y_r \\ Z_r \end{Bmatrix}$$

(b) Displacement transformation

Figure 5. Relating the acceleration measurement points to the DOFs of analytical model.

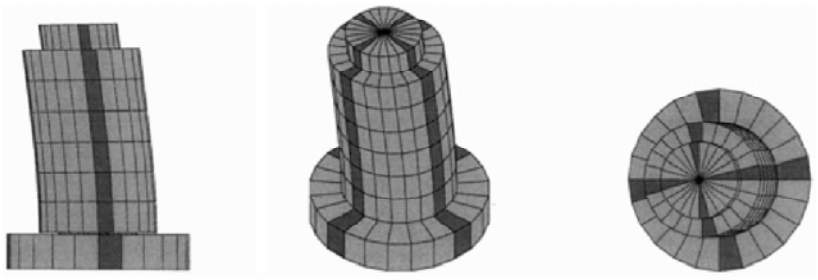

(a) X-Z plane (b) 3D view (c) X-Y plane

Figure 6. The first bending mode from Model 1: 26.55 Hz.

5. APPLICATION TO DAMAGE DETECTION

This section illustrates the Bayesian probabilistic approach for the detection of the plastic hinge location in the column tested. The natural frequencies and modal vectors estimated after each cyclic load test corresponding to Δy, $1.5\Delta y$, $2.5\Delta y$, $4.0\Delta y$ and $7.0\Delta y$ (Tests 1, 2, 3, 4 and 5, respectively) are employed for damage diagnosis of the column. This incremental loading caused continuous stiffness deterioration of the column structure and simulated the condition for

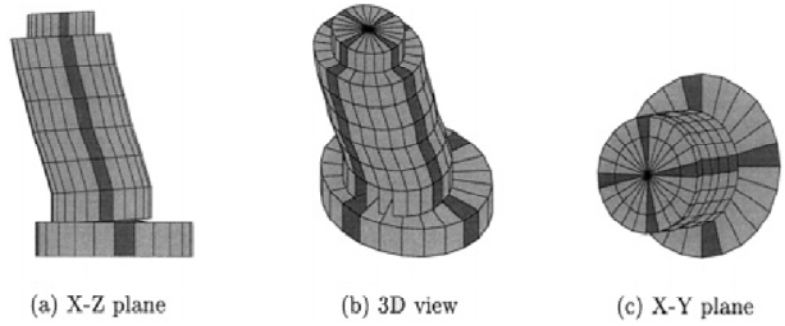

Figure 7. The first bending mode from test data: 27.82.

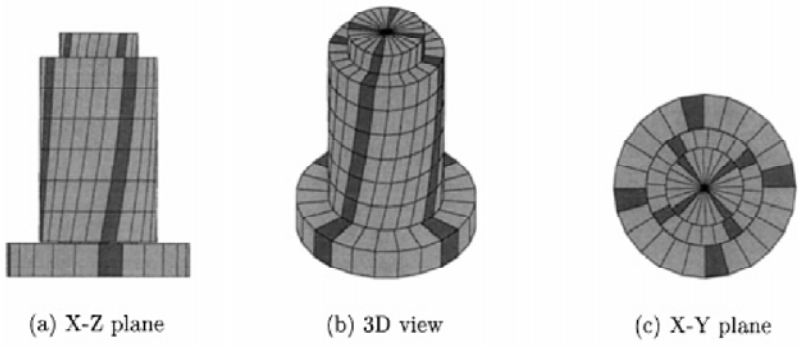

Figure 8. The first torsion model from Model 1: 115.87 Hz.

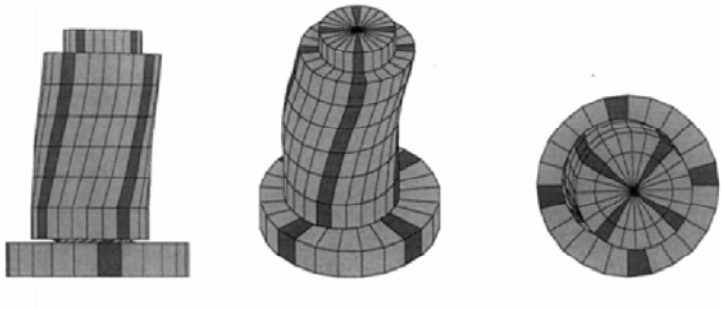

Figure 9. The first torsion mode from test data: 110.42 Hz. (a) X-Z plane; (b) 3D view; (c) X-Y plane.

continuous monitoring. Table II shows the natural frequencies of the first bending and the first torsional modes at each displacement level. Note that only the first two modes are employed for damage detection since only the first two modes are reliably estimated from the experimental FRFs, and the discrepancies between the analytical modal vectors and the measured modal

Table II. Natural frequency (Hz) estimated at different displacement levels.

Mode	Initial	Δy	$1.5\,\Delta y$	$2.5\,\Delta y$	$4.0\,\Delta y$	$7.0\,\Delta y$
1st bending	27.82	12.80	7.31	6.15	5.61	5.21
1st torsion	110.42	109.97	50.20	36.90	20.32	19.04

vectors become larger for higher modes. Deformation of plastic hinge was observed near the connection region between the foundation and the retrofitted portion of the column. It appears that this plastic hinge deformation was mainly responsible for the significant decreases in the first bending and torsional modes. This damage region approximately corresponds to elements 2 and 3 of the analytical models in Figures 3 and 4.

The measured and analytical modal vectors are normalized with respect to the analytical mass matrix. Each beam element is defined as a substructure in this example. This study mainly de monstrates the continuous updating feature of the Bayesian approach. Starting from a uniform prior probability, $P(H_j)$, for every element (substructure), the posterior damage probability, $P(\mathrm{H}_j|\hat{\Psi}_{N_s})$, is updated using Equation (4) when new modal parameters, $\hat{\Psi}_{N_s}$, are estimated after each cyclic load test. Also, damage is assumed to lie within a single element (substructure). For the examples presented here, we use an incremental step $\Delta\theta = 0.05$. In addition, a value of 0.9 is used for the damage threshold θ^* for every substructure; that is, an over 10 per cent decrease in the stiffness is defined as *damage*.

5.1. *Damage detection using the Bayesian probabilistic approach*

First, damage diagnosis is conducted using the first analytical model (Model 1). Sub-structures near the actual damage locations are shaded with darker color in Figures 10 and 11, respectively. The diagnosis results shown in Figures 10 and 11 are obtained by updating the damage probabilities either continuously or separately using the modal parameters measured at different deformation levels.

1. Figure 10 shows the continuous update of the damage probabilities using Model 1. Subtitles 'Update i' ($i = 1, 2, \ldots, 5$) in Figure 10 indicates that the corresponding damage probabilities are updated using modal parameters from Tests 1, 2, ..., i. Figure 10 shows that the diagnosis result improves as more data sets are employed for damage detection.
2. For comparison, Figure 11 presents the diagnosis results obtained by using each individual data set separately. Subtitles 'Test i' ($i = 1, 2, \ldots, 5$) in Figure 11 indicate that the corresponding damage probabilities are computed solely by using the modal parameters from Test i. When modal parameters from Tests 2 and 3 are employed separately (the counterparts to the figures with subtitles Update 2 and Update 3 in Figure 10), the proposed method missed the actual damage locations. While the figures with subtitles Update 2 and Update 3 in Figure 10 identify the third substructure as the most probable damage location.

In both cases, the third substructure is diagnosed as the most likely damage location at the end of the damage detection process. However, more strictly speaking, the actual plastic hinge was observed near the region where Elements 2 and 3 adjoint each other. To investigate if the proposed method approaches the hinge location, another model with finer beam elements

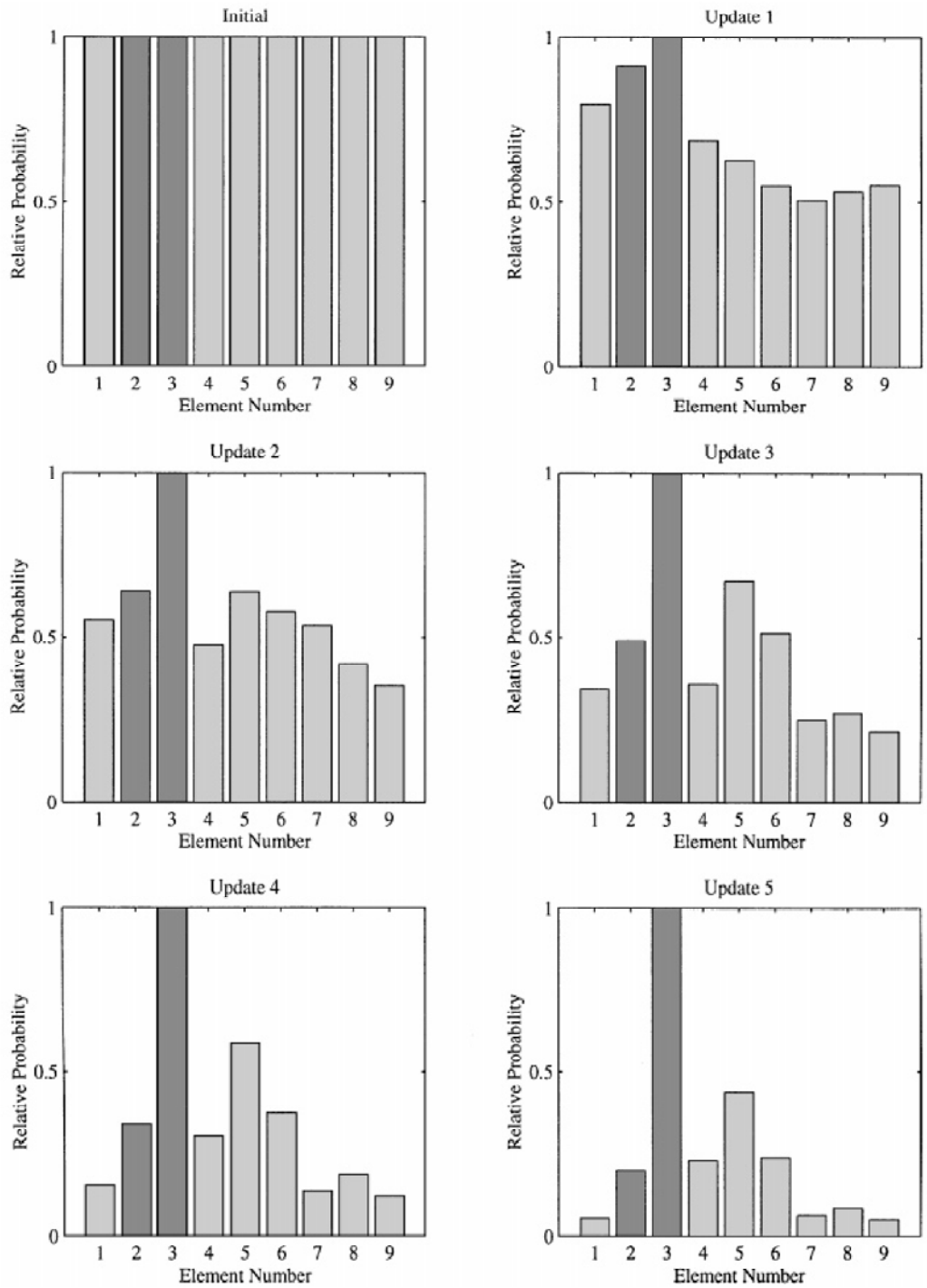

Figure 10. The damage probabilities after continuous updating (using Model 1).

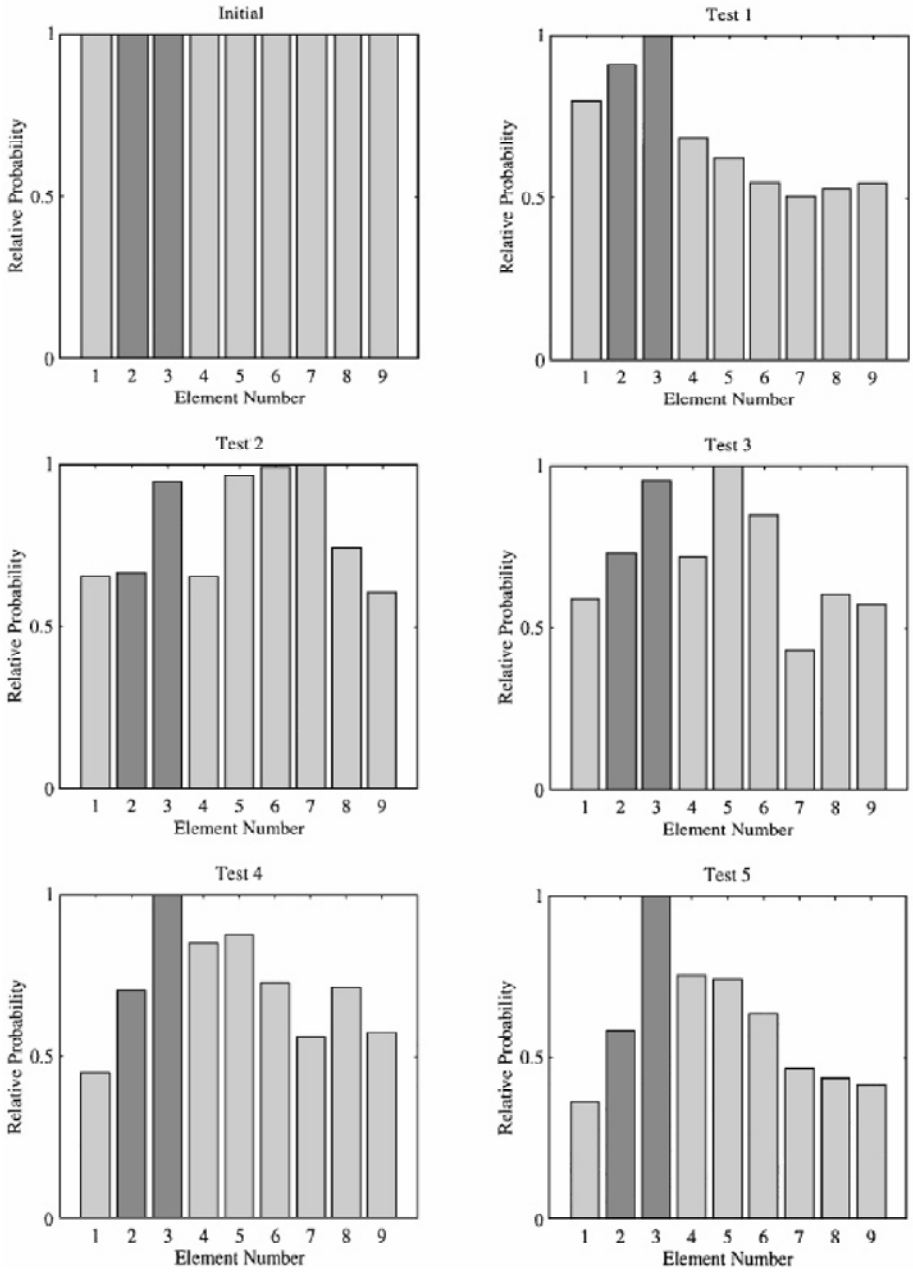

Figure 11. The damage probabilities computed from individual data set (using Model 1).

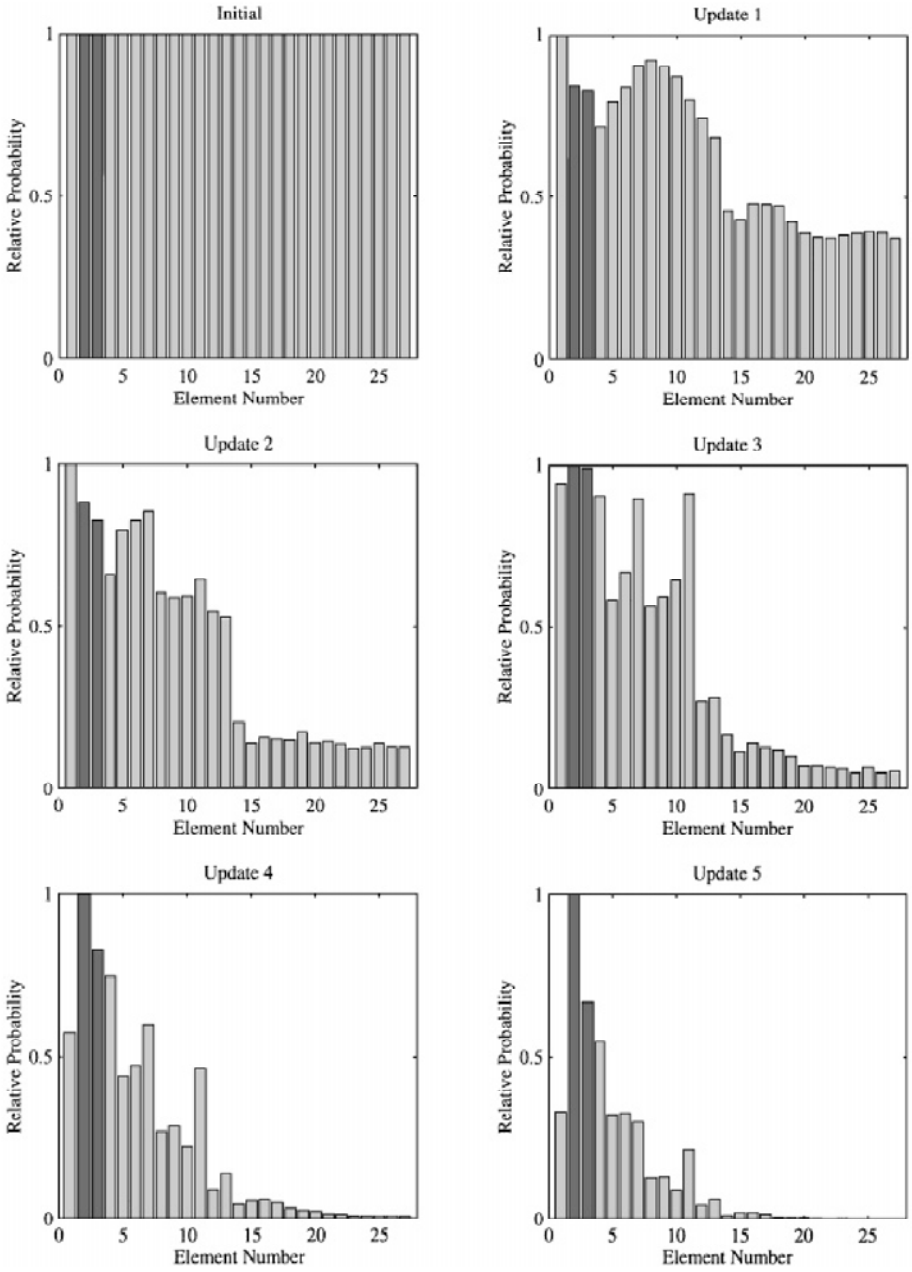

Figure 12. The damage probabilities after continuous updating (using Model 2).

(Model 2) is employed next. All other conditions except the model remain the same as in the previous diagnosis. While Model 1 has 9 elements, Model 2 consists of 27 elements to represent the test column. Figures 12 and 13 again illustrate that the diagnosis using the proposed Bayesian

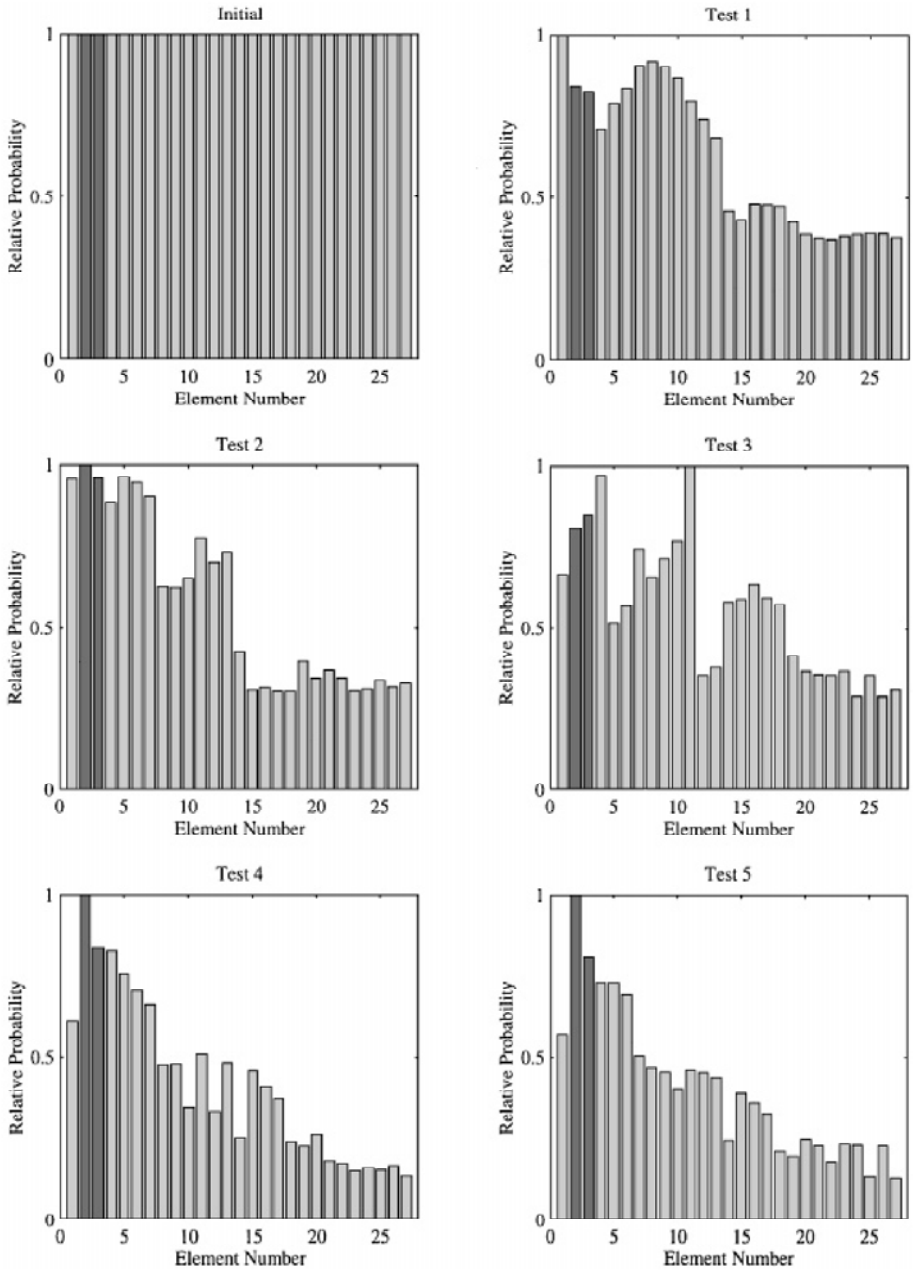

Figure 13. The damage probabilities computed from individual data set (using Model 2).

Table III. Estimated damage amount $(1 - \theta_i)$ at different damage stage.

	Test 1 (%)	Test 2 (%)	Test 3 (%)	Test 4 (%)	Test 5 (%)
Model					
$1-\theta_2$	38	83	87	83	89
$1-\theta_3$	60	69	90	80	88
Model 2					
$1-\theta_2$	59	88	92	87	92
$1-\theta_3$	72	78	94	91	93

approach converges to the actual damage locations (the actual damaged elements are distinguished by darker colour in the figures). At the end of the updating, the diagnosis result clearly shows that the column was very likely damaged between the top of the foundation and the bottom of the retrofit jacket.

The comparison of individual and continuous updating shows that the proposed Bayesian framework systematically combines the existing data with newly obtained data and the continuous updating is more stable in a sense that it is less sensitive to a single data set, and extracts consistent trends among the accumulated data. Furthermore, to provide information regarding the degree of damage for different damage stage, the values of the substructure stiffness reduction $(1 - \theta_i)$ at each damage stage are estimated from continuous updating and are reported in Table III for the actual damage locations (the second and third substructures). Continuous stiffness deterioration is observed in the actual damage locations (the second and third substructures).

5.2. *Damage detection using deterministic approaches*

Two deterministic model updating or damage detection schemes are applied to the same test data of the column structure in order to compare the proposed probabilistic approach with some existing deterministic approaches. A sensitivity-based element-by-element (SB-EBE) method proposed by Hemez [2] and a minimum rank perturbation theory (MRPT) proposed by Kaouk and Zimmerman [1] are employed in this study as examples to deterministic approaches. Both methods can be categorized as model-based methods that utilize estimated modal properties for damage diagnosis. The detailed development of these methods are described in References [1, 2].

First, the SB-EBE method is applied to the experimental test data (Tests 1–5). This method was not successful in locating damage regions for all 5 test cases. Therefore, the diagnosis results are not presented in this paper. Next, the MRPT is applied to the experimental data. The MRPT does not directly identify damage at the element levels. The MRPT method estimates only the 'damaged' DOFs that correspond to large dynamic residuals. Then, an analyst should infer the damaged elements based on the connectivity information of the structure. When the experimental data (Tests 1–5) are employed, the damaged DOFs are not clearly noticeable until the last data set (Test 5) is used. Figure 14 shows the diagnosis result when Test 5 data are employed. The DOFs 1–18 correspond to Elements 2 and 3 are assumed to be damaged. Again, the actual damaged DOFs are distinguished by darker color in Figure 14. Figures 14(a) and 14(b) show the normalized dynamic residual from the first bending and torsional models, respectively. The *orthogonal procrustes* technique in Reference [18] is employed for the mode shape expansion.

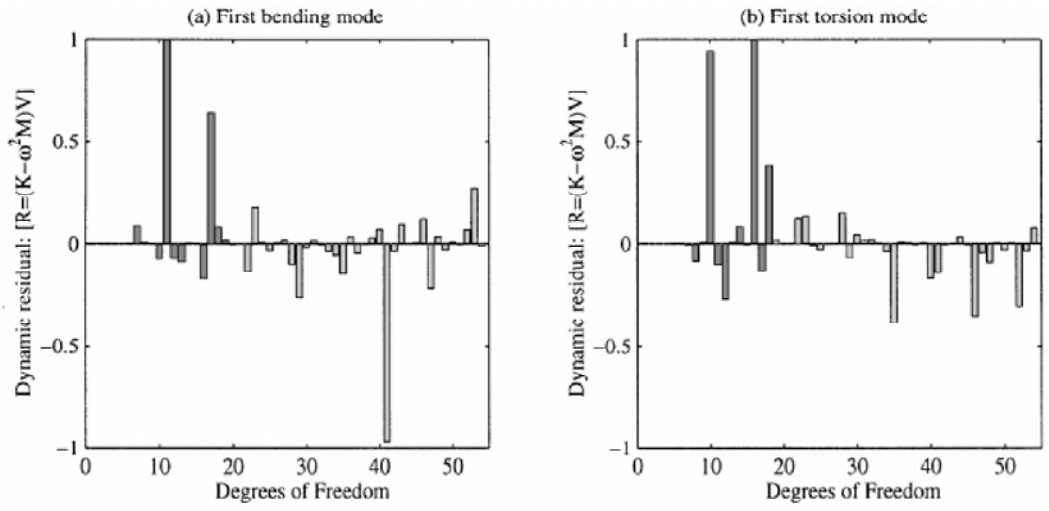

Figure 14. Damage diagnosis using MRPT: experimental example.

Note that when mode shape expansion techniques (component mode synthesis [19] and modal co-ordinate expansion [20]) other than the orthogonal procrustes expansion [18] are employed, the damaged DOFs are not clearly indicated. The selection of mode shape expansion techniques seems to be an essential factor for the success of damage diagnosis.

The poor performance of the two deterministic approaches can be attributed to the following:

1. Most mode shape expansion techniques including the ones used in this paper expand the measured modal vectors to the size of the analytical model based on the measurements at the instrumented DOFs and the corresponding analytical stiffness and mass matrices. These techniques work only when the analytical model is already a good representation of the structure. Mode shape expansion techniques generally do not produce the expanded modal vectors that are accurate enough to provide reliable information about damage. As previously mentioned, the discrepancy between the analytical model and the test data was large even in the initial stage. This discrepancy produced additional errors into the two deterministic approaches presented. (Note that, the proposed Bayesian approach does not require any mode shape expansion or model reduction procedures.)
2. Both deterministic approaches basically update the system stiffness matrix so as to minimize the dynamic force residuals. However, for the frame structures as the one presented here, the order of magnitudes for the residual forces in rotational DOFs is significantly larger than that of translational DOFs. Therefore, the residual forces in the rotational DOFs are generally weighted more than those corresponding to the translational DOFs. The difference in magnitude of residual force for each DOF contributed to the poor performance of the deterministic approaches.

Alvin [21] addresses some of the aforementioned problems by employing dynamic displacement residuals, rather than force residuals. Furthermore, the Bayesian estimate is introduced to the SB-EBE method to incorporate the relative confidence measures for the parameters being

updated and the test data used for updating. It would be an interesting research task to compare this approach with the one described in this paper.

6. SUMMARY AND DISCUSSIONS

A Bayesian approach is applied to detect the location of plastic hinge deformation of the reinforced-concrete bridge column, which is constructed and tested at the University of California, Irvine. In the cyclic load tests, the column is statically pushed with incremental lateral displacement until a plastic hinge is fully formed at the bottom portion of the column, and the vibration tests are performed at different damage stages. The static cyclic load test of the column structure is conducted in a displacement incremental manner until a plastic hinge is fully formed at the bottom end of the column. This incremental loading simulates the continuous deterioration of the structure. Furthermore, the vibration tests are conducted after each cyclic test is performed at different displacement levels. The modal parameters estimated from the vibration tests of different damage levels are used to continuously update the damage probabilities.

Two analytical models with simple beam elements are constructed as the analytical models for damage detection. The proposed damage detection method was able to locate the damaged region using simplified analytical models, although (1) only the first bending the first torsional modes are estimated from experimental test data, (2) the locations where the accelerations are measured do not coincide with the degrees of freedom of the analytical model, and (3) discrepancies exist between the undamaged test structure and the analytical model. Furthermore, the proposed Bayesian approach distinguishes itself with other deterministic damage detection methods in that the framework of the Bayesian approach is particularly suitable to continuous monitoring of structures. Other similar Bayesian-based approach for continuous monitoring has also been proposed [22]. The Bayesian framework enables systematic updating of damage probabilities when new test data become available, and results in better diagnosis by employing multiple data sets than just by using each test data set separately.

ACKNOWLEDGEMENTS

The first author wishes to express his sincere thanks to Professor Gerard C. Pardoen and his students at the University of California at Irvine for providing an opportunity to observe the bridge column test. Also, the authors are indebted to Dr Charles R. Farrar and Dr Scott W. Doebling of the Los Alamos National Laboratory for providing the vibration test data. This research was partially sponsored by the National Science Foundation under Grant No. CMS-95261-2.

REFERENCES

1. Kaouk M, Zimmerman DC. Structural damage assessment using a generalized minimum rank perturbation theory. *American Institute of Aeronautics and Astronautics* 1994; **32**: 836–842.
2. Hemez FM. Theoretical and experimental correlation between finite element models and modal tests in the context of large flexible space structures. *Ph.D. Thesis*, Aerospace Engineering Sciences, University of Colorado, Boulder, CO, 1993.
3. Smith SW. Damage detection and location in large space trusses. *Ph.D. Thesis*, Department of Aerospace and Ocean Engineering, Virginia Polytechnic Institute and State University, Blacksburg, VA, 1988.

4. Wood MG. Damage analysis of bridge structures using vibrational techniques. *Ph.D. Thesis*, Department of Mechanical and Electrical Engineering, University of Aston, Birmingham, Birmingham, UK, 1992.
5. Farrar CR, Deobling SW, Cornewll PJ, Straser EG. Variability of modal parameters measured on the Alamosa Canyon Bridge. In *Proceedings of the 15th International Modal Analysis Conference*, Orlando, FL, 1997; 257–263.
6. Sohn H, Dzwonczyk M, Straser EG, Kiremidjian AS, Law KH, Meng TH. An experimental study of temperature effect on modal parameters of the Alamosa Canyon Bridge. *Earthquake Engineering and Structural Dynamics* 1999; **28**: 879–897.
7. Baruch M. Optimization procedure to correct stiffness and flexibility matrices using vibration tests. *American Institute of Aeronautics and Astronautics* 1978; **16**: 1208–1210.
8. Kammer DC. Optimum approximation for residual stiffness in linear system identification. *American Institute of Aeronautics and Astronautics* 1988; **26**: 104–112.
9. Kabe AM. Stiffness matrix adjustment using mode data. *American Institute of Aeronautics and Astronautics* 1985; **23**: 1431–1436.
10. Smith SW, Beattie CA. Secant-method adjustment for structural models. *American Institute of Aeronautics and Astronautics* 1991; **29**: 119–126.
11. Beck JL, Katafygiotis LS. Updating models and their uncertainties. I: Bayesian statistical framework. *Journal of Engineering Mechanics, ASCE* 1998; **124**: 455–461.
12. Katafygiotis LS, Beck JL. Updating models and their uncertainties. II: Model identifiability. *Journal of Engineering Mechanics, ASCE*, 1998; **124**: 463–467.
13. Sohn H, Law KH. Bayesian probabilistic approach for structure damage detection. *Earthquake Engineering and Structural Dynamics* 1997; **26**: 1259–1281.
14. Sohn H, Law KH. Application of load-dependent Ritz vectors to Bayesian probabilistic damage detection. *Probabilistic Engineering Mechanics* 2000; **15**: 139–153.
15. Yuen KV. Structural modal identification using ambient dynamic data. *MPhil Thesis*, Department of Civil Engineering, Hong Kong University of Science and Technology, Hong Kong, 1999.
16. Katafygiotis LS, Lam HF. A probabilistic framework for structural health monitoring. In *Proceedings of the 12th Engineering Mechanics Conference, ASCE*, La Jolla, CA, 1998; 1379–1382.
17. Katafygiotis, LS, Papadimitriou C, Lam HF. A probabilistic approach to structural model updating. *Soil Dynamics and Earthquake Engineering* 1998; **17**: 495–507.
18. Smith SW, Beattie CA. Simultaneous expansion and orthogonalization of measured modes for structure identification. *Technical Report AIAA*-90-1218-CP, American Institute of Aeronautics and Astronautics, 1990.
19. Berger H, Chaquin JP, Ohayon R. Finite element model adjustment using experimental data. In *Proceedings of the 2nd International Modal Analysis Conference,* Orlando, FL, 1984; 638–642.
20. Imregun M, Ewins DJ. An investigation into mode shape expansion techniques. In *Proceedings of the 11th International Modal Analysis Conference*, Kissimmee, FL, 1993; 168–175.
21. Alvin KF. Finite element model update via Bayesian estimation and minimization of dynamic residuals. *American Institute of Aeronautics and Astronautics*, 1997; **35**: 879–886.
22. Vanik MW. A Bayesian probabilistic approach to structural health monitoring. *Ph.D. Thesis*, Applied Mechanics Department, California Institute of Technology, Pasadena, CA, 1997.

